MEEN 612 Project 1
Kinematics, Dynamics and Control of a 2-Link Planar Robot

Jay Shah

November 23, 2020

Abstract

A 2-link planar robotic manipulator is analyzed and its forward and reverse kinematics is performed. Further, through inverse kinematics, joint variables in joint-angles space have been deduced from desired locations in the ground co-ordinate frame and a smooth trajectory with zero jerk is constructed through interpolation, with available motor torques constraint in mind. Then, PD Controller, Modified Computed Torque Controller and Adaptive Controllers have been designed and their performance are analyzed and inferences have been made from the observations. Tracking errors have been plotted along with input torques for each controller and conclusions are drawn at the end of the report from these plots.

Desired Trajectory

It is given that the robot must pass through the points (0.48,0.1), (0.38,0), (0.48,0.1) and (0.58,0) in the same sequence as mentioned. The co-ordinates given are the co-ordinates of the end-effector of the robot in ground frame. The robot is shown in Fig.1. The length of the links are $L_1 = 0.38$m and $L_2 = 0.24$m. The inertial parameters are $p_1 = 3.4$, $p_2 = 0.4$, $p_3 = 0.3$ at zero payload condition.

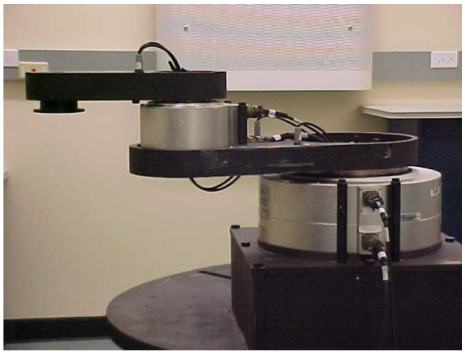

Figure 1: 2-Link Planar Robot

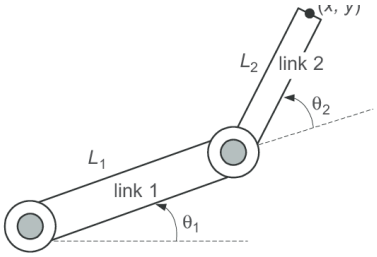

Figure 2: 2-Link Planar Robot Top View Schematic

The schematic of the robotic arm can be seen in Fig.2. θ_1 and θ_2 are the joint angles. It can be easily seen from

the geometry in Fig.2 that the forward kinematics of the robotic arm, i.e., the co-ordinates of the end-effector of the robotic arm in ground frame can be given as follows,

$$\begin{bmatrix} x \\ y \end{bmatrix} = \begin{bmatrix} L_1 cos\theta_1 + L_2 cos(\theta_1 + \theta_2) \\ \mathrm{L_1 sin}\theta_1 + L_2 \mathrm{sin}(\theta_1 + \theta_2) \end{bmatrix} \tag{1}$$

Squaring and adding the 2 rows in equation 1, we have the following equation,

$$x^2 + y^2 = L_1^2 cos^2\theta_1 + L_2^2 cos^2(\theta_1 + \theta_2) + 2L_1 L_2 \mathrm{cos}\theta_1 \mathrm{cos}(\theta_1 + \theta_2) + L_1^2 sin^2\theta_1 + L_2^2 sin^2(\theta_1 + \theta_2) + 2L_1 L_2 sin\theta_1 sin(\theta_1 + \theta_2)$$

$$\Rightarrow \qquad \theta_2 = \pm cos^{-1}\left(\frac{x^2 + y^2 - L_1^2 - L_2^2}{2L_1 L_2}\right) \tag{2}$$

Thus, there are at most 2 values of θ_2. Substituing θ_2 in equation 1, θ_1 can be found. By solving the equation, $\mathrm{sin}\theta_1$ and $\mathrm{cos}\theta_1$ are found and θ_1 can be found using the arc-tangent function in MATLAB.

$$\therefore \qquad \theta_1 = atan2(sin\theta_1, cos\theta_1) \tag{3}$$

Thus, the inverse kinematics is done, and θ_1 and θ_2 can be found if the co-ordinates of the end-effector are given in the ground frame. There are at most 2 possible pairs of (θ_1,θ_2) for each given position of the end-effector. By calculating the joint angles based on the given co-ordinates of the desired trajectory, an interpolation for generation of a smooth function can be done in the joint-space. Table 1 shows the values of co-ordinates and the corresponding joint angle values.

Table 1: Joint Angles

Co-ordinates of End-Effector (x, y)	Joint Values (θ_1, θ_2)
(0.48, 0.1)	(-0.2936, 1.3587), (0.7044, -1.3587)
(0.38, 0)	(-0.6426, 1.8921), (0.6426, -1.8921)
(0.48, -0.1)	(-0.7044, 1.3587), (0.2936, -1.3587)
(0.58, 0)	(-0.2835, 0.7424), (0.2835, -0.7424)

Assuming the joint variables to be the first pair from Table 1 for each point, Hermite interpolation is performed to construct a smooth trajectory, with the boundary conditions and derivatives at end points of the trajectory and a few intermediate points. Also, it is given that the trajectory period is of 4s and is repeated periodically, and the time for point to point motion is equally distributed. Therefore, it would take 1s to reach at the next point from the current point. The conditions on θ_1 and θ_2 can be given as follows,

$\theta_1(0)$ = -0.2936; $\dot{\theta_1}(0) = 0$; $\ddot{\theta_1}(0) = 0$; $\dddot{\theta_1}(0) = 0$; $\theta_1(1)$ = -0.6426; $\theta_1(2)$ = -0.7044; $\theta_1(3)$ = -0.2835;
$\theta_1(4)$ = -0.2936; $\dot{\theta_1}(4) = 0$; $\ddot{\theta_1}(4) = 0$; $\dddot{\theta_1}(4) = 0$;

$\theta_2(0)$ = 1.3587; $\dot{\theta_2}(0) = 0$; $\ddot{\theta_2}(0) = 0$; $\dddot{\theta_2}(0) = 0$; $\theta_2(1)$ = 1.8921; $\theta_2(2)$ = 1.3587; $\theta_2(3)$ = 0.7424;
$\theta_2(4)$ = 1.3587; $\dot{\theta_2}(4) = 0$; $\ddot{\theta_2}(4) = 0$; $\dddot{\theta_2}(4) = 0$;

Hence, it can be seen that there are 11 conditions needed to be satisfied for each θ_1 and θ_2. Therefore, a hermite polynomial of 10^th order is required. It can be seen in equations 4 and 5.

$$\theta_1 = \alpha_0 + \alpha_1 t + \alpha_2 t^2 + \alpha_3 t^3 + \alpha_4 t^4 + \alpha_5 t^5 + \alpha_6 t^6 + \alpha_7 t^7 + \alpha_8 t^8 + \alpha_9 t^9 + \alpha_{10} t^{10} \tag{4}$$

$$\theta_2 = \beta_0 + \beta_1 t + \beta_2 t^2 + \beta_3 t^3 + \beta_4 t^4 + \beta_5 t^5 + \beta_6 t^6 + \beta_7 t^7 + \beta_8 t^8 + \beta_9 t^9 + \beta_{10} t^{10} \tag{5}$$

We have 11 equations and 11 unknown variables for each, θ_1 and θ_2. Solving these systems of equations would give the values of α_i and β_i. Thus, θ_1 and θ_2 can be expressed as,

$$\theta_1 = -0.2936 - 2.04t^4 + 3.11t^5 + 1.95t^6 + 0.65t^7 - 0.12t^8 + 0.01t^9 - 0.00048t^{10} \tag{6}$$

$$\theta_2 = 1.3587 + 3.19t^4 - 4.4t^5 + 2.32t^6 - 0.54t^7 + 0.04t^8 + 0.003t^9 - 0.00051t^{10} \tag{7}$$

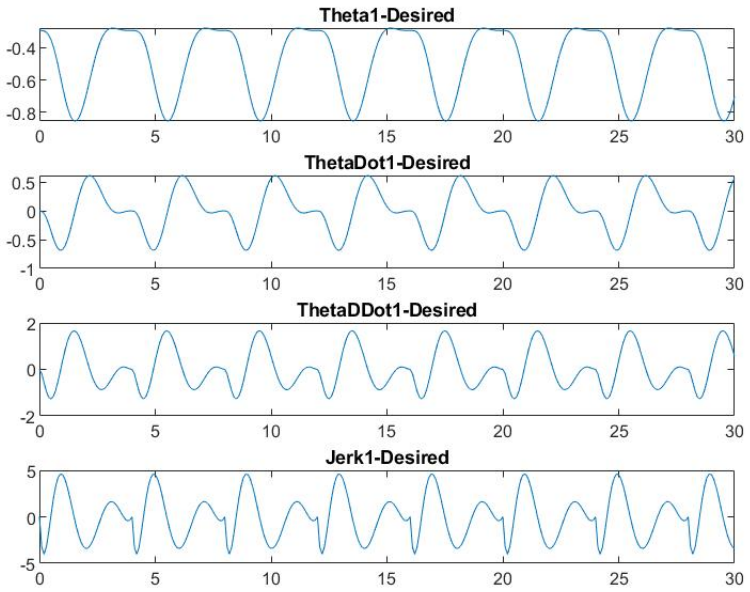

Figure 3: Trajectories of θ_1

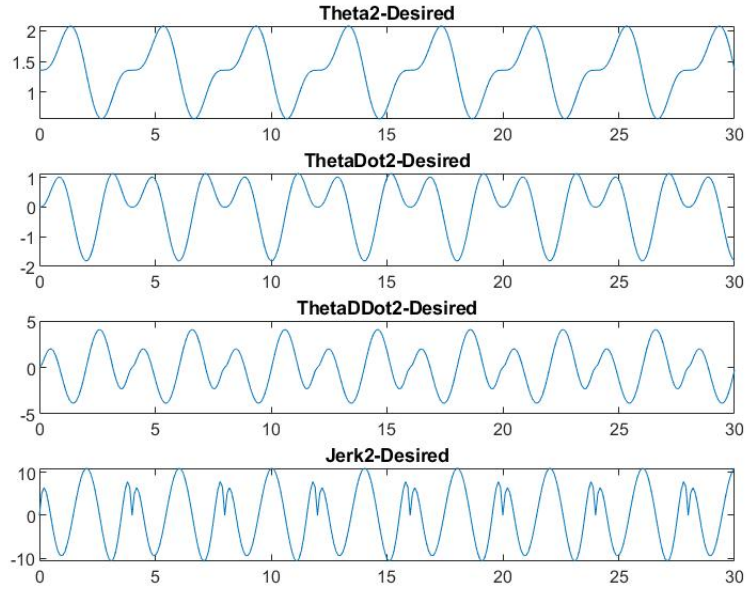

Figure 4: Trajectories of θ_2

The plots of θ_1 and θ_2 and their derivatives can be seen in Fig.3 and Fig.4 respectively. It can be seen that the trajectories and their derivatives are smooth and continuous. Also, they satisfy all the 11 conditions. In Fig.5, the trajectory of link 1 and link 2 in the x-y plane can be seen.

The maximum available torques for base and elbow motors are 240 N-m and 40 N-m respectively. It needs to be verified that the generated trajectory demands the desired torque that is less than the available torque of the motors. Therefore, the following condition needs to be satisfied,

$$M(\theta)\ddot{\theta} + C(\theta, \dot{\theta}) \leq \tau_{available}$$

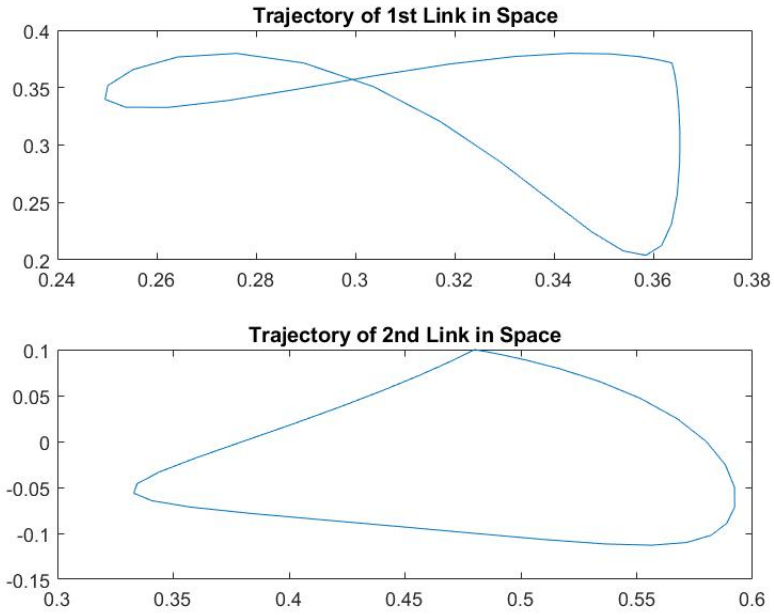

Figure 5: Trajectories of both links

Also,

$$M(\theta) = \begin{bmatrix} p_1 + 2p_3\cos(\theta_2) & p_2 + p_3\cos(\theta_2) \\ p_2 + p_3\cos(\theta_2) & p_2 \end{bmatrix}$$

$$C(\theta, \dot{\theta}) = \begin{bmatrix} -p_3\dot{\theta_2}\sin(\theta_2) & -p_3(\dot{\theta_1} + \dot{\theta_2})\sin(\theta_2) \\ p_3\dot{\theta_1}\sin(\theta_2) & 0 \end{bmatrix}$$

The calculated torque values have been plotted against time in Fig.6 and it can be clearly seen that the desired torque values for both the joints are below the available rate motor torques.

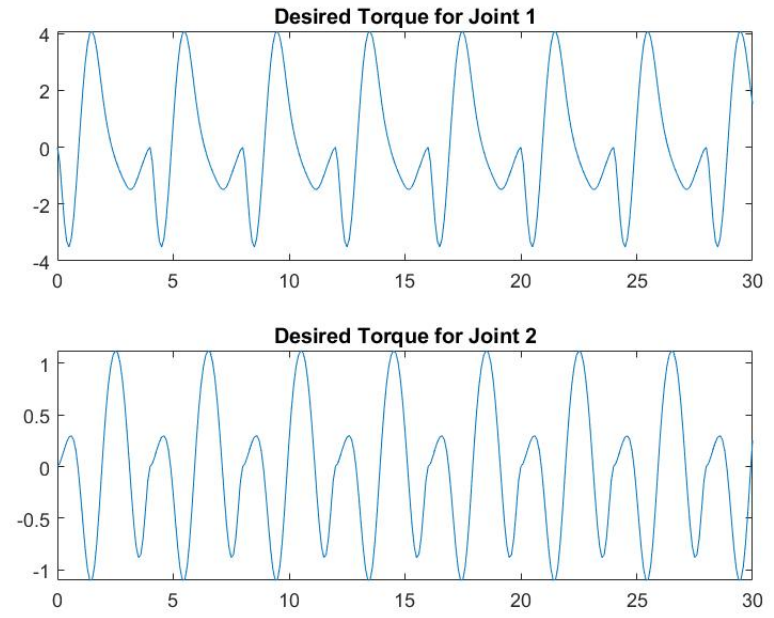

Figure 6: Desired Torque Values

PD Control

Proportional-Derivative Controller is one of the controllers used in tracking control in robots. Errors in position and its differentiation, i.e., errors in velocity are fed back to the system with some gains multiplied with them. The mathematical expression for the input torque τ can be written as,

$$\tau = M(\theta)\ddot{\theta}_{des} + C(\theta, \dot{\theta})\dot{\theta}_{des} - K_p e_p - K_d \dot{e}_p \tag{8}$$

where $\ddot{\theta}_{des}$ and $\dot{\theta}_{des}$ are desired quantities and its expression is derived through interpolation in the Desired Trajectories section. $e_p = \theta$ - θ_{des} and $\dot{e}_p = \dot{\theta}$ - $\dot{\theta}_{des}$ are the errors in position and velocity respectively. The main purpose of using a controller is to ensure that e_p and $\dot{e}_p$ converge to zero asymptotically. This can be showed mathematically by the help of Lyapunov's stability theorem. An energy like function is defined for the system an which is called a Lyapunov function candidate, such that it's derivative is negative definite, implying that the energy like value of the system decreases over time, and as a result, the errors converge to zero. One such Lyapunov function candidate is given by,

$$V = \frac{1}{2}\dot{e}_p^T M(\theta)\dot{e}_p + \frac{1}{2}e_p^T K_p e_p \tag{9}$$

$$\text{Time derivative of V, } \dot{V} = \dot{e}_p^T M(\theta)\ddot{e}_p + \frac{1}{2}\dot{e}_p^T \dot{M}(\theta)\dot{e}_p + e_p^T K_p \dot{e}_p$$

Simplifying the above equation,

$$\dot{V} = -\dot{e}_p^T K_d \dot{e}_p \tag{10}$$

For V to be a Lyapunov function candidate, it has to be a positive definite function. Thus, K_p has to be positive definite. Also, K_d has to be positive definite to make $\dot{V}$ to be semi-negative definite. Further, by LaSalle's theorem, it can be proved that $\dot{V} = 0$ if and only if $\dot{e}_p = 0$. Thus, $\dot{V}$ is negative-definite and as a result, e_p and $\dot{e}_p$ converge to zero.

The gain matrices used for the simulation are,

$$K_p = \begin{bmatrix} 350 & 0 \\ 0 & 300 \end{bmatrix}, \quad K_d = \begin{bmatrix} 40 & 0 \\ 0 & 50 \end{bmatrix}$$

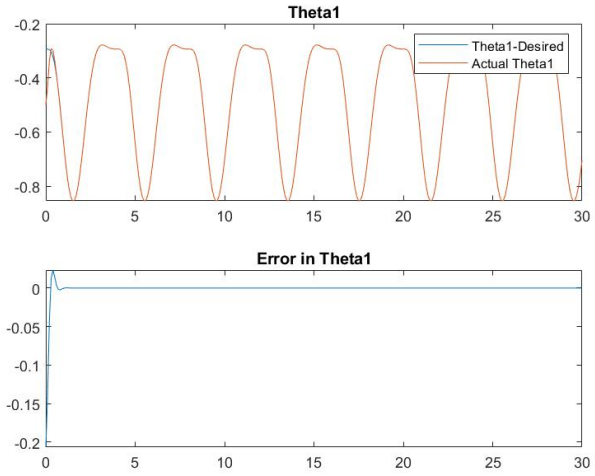

Figure 7: Actual, Desired and Error Plots of θ_1

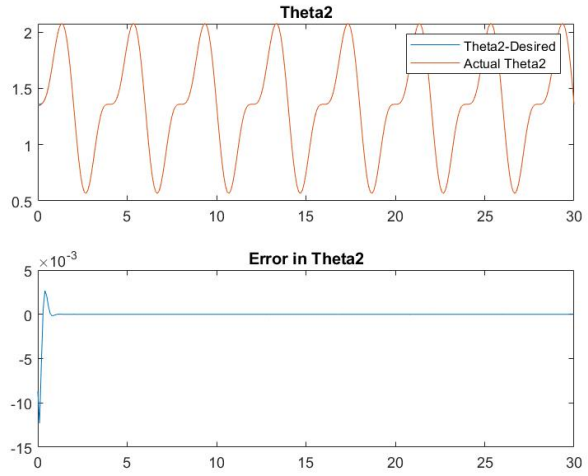

Figure 8: Actual, Desired and Error Plots of θ_2

Fig.7 and Fig.8 show the convergence of joint angles θ_1 and θ_2 to their desired value and their errors over the simulation time respectively. Also, Fig.9 and Fig.10 show the similar plot for joint velocities $\dot{\theta_1}$ and $\dot{\theta_2}$ respectively. Fig.11 shows the input torques τ_1 and τ_2. It can be seen that there is a high requirement of input torque for both the motors because of the initial error. After the convergence, both τ_1 and τ_2 are significantly lower than the initial values.

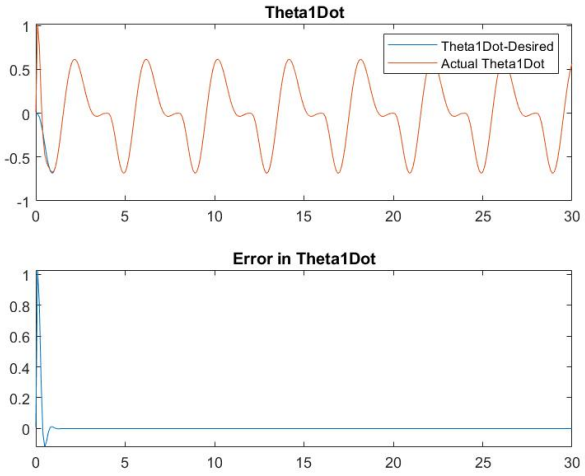

Figure 9: Actual, Desired and Error Plots of $\dot{\theta_1}$

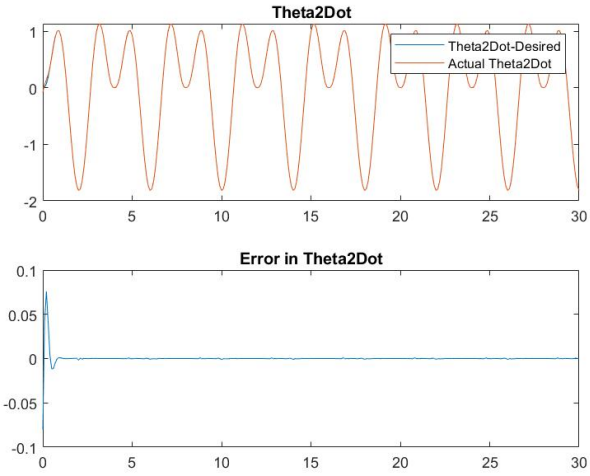

Figure 10: Actual, Desired and Error Plots of $\dot{\theta_2}$

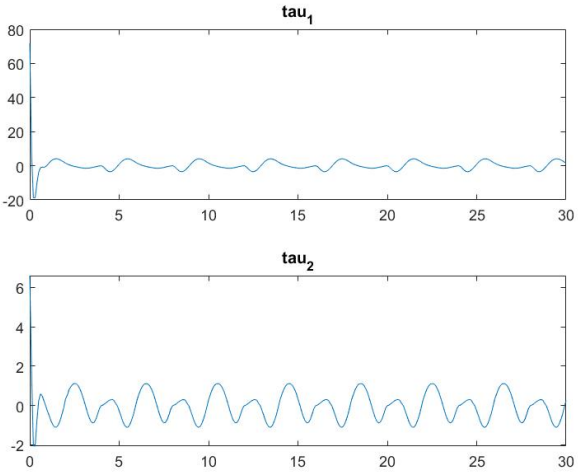

Figure 11: Input torques for both motors

Modified Computed Torque Controller

While the PD Controller works perfectly fine as can be seen in the previous section, the modified computed torque controller (CTC) uses a linear function whose bound and negative derivative guarantees the convergence of errors to zero. One such linear function can be the composite error S which can be given as,

$$S = \dot{e}_p + \lambda e_p$$

where λ is a constant which can be considered as a damping constant of the system. Additionally, a reference velocity is introduced which is defined as follows.

$$\dot{\theta}_r = \dot{\theta}_{des} - \lambda(\theta - \theta_{des})$$

The Lyapunov function candidate is defined as follows in this case,

$$V = \frac{1}{2} S^T M(\theta) S$$

$$\Rightarrow \dot{V} = S^T[M(\theta)\dot{S} + C(\theta,\dot{\theta})S] \tag{11}$$

$$= S^T[M(\theta)\ddot{\theta} + C(\theta,\dot{\theta})\dot{\theta} - M(\theta)\ddot{\theta}_r - C(\theta,\dot{\theta})\dot{\theta}_r] \tag{12}$$

$$= S^T[\tau - M(\theta)\ddot{\theta}_r - C(\theta,\dot{\theta})\dot{\theta}_r] \tag{13}$$

In order to converge the errors to zero, $\dot{V}$ has to be negative definite. Thus, τ can be defined as,

$$\tau = M(\theta)\ddot{\theta}_r + C(\theta, \dot{\theta})\dot{\theta}_r - KS$$

K is the gain matrix and it is a positive definite matrix.

$$\therefore \dot{V} = -S^T KS$$

It can be observed that for V to be a Lyapunov function candidate, it has to be positive definite. Thus $V = 0$ if and only if $S = 0$. Thus, $-S^T KS = 0$ if and only if $S = 0$. Further, K is positive definite. Thus, $S^T KS < 0$. As a result, $\dot{V} < 0 \Rightarrow V \to 0 \Rightarrow e_p \to 0$ & $\dot{e}_p \to 0$.

It can be noted that the composite error S has the unit of velocity. Therefore, the values of the gain matrix K have been picked same as the values of gain matrix K_d in the PD controller. This is done to have a fair comparison of the convergence results from both the controllers. Thus, the K matrix is as follows,

$$K = \begin{bmatrix} 40 & 0 \\ 0 & 50 \end{bmatrix}$$

The plots from the simulation are shown below. Fig.12, Fig.13, Fig.14 and Fig.15 show the convergence plot of the state variables θ_1, θ_2, $\dot{\theta}_1$ and $\dot{\theta}_2$ respectively. Fig.16 shows the plot of input torques τ_1 and τ_2 over the time period of 30s.

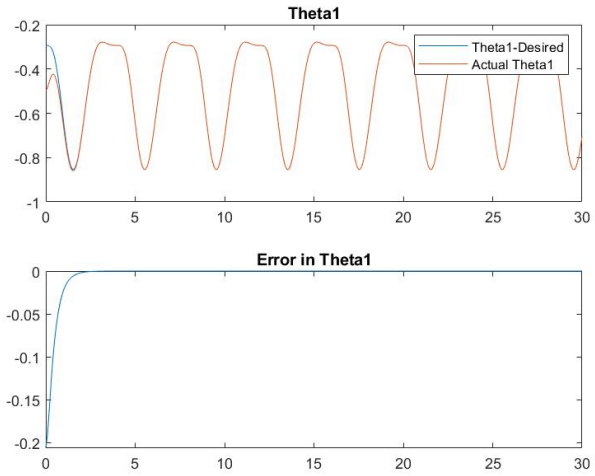

Figure 12: Actual, Desired and Error Plots of θ_1

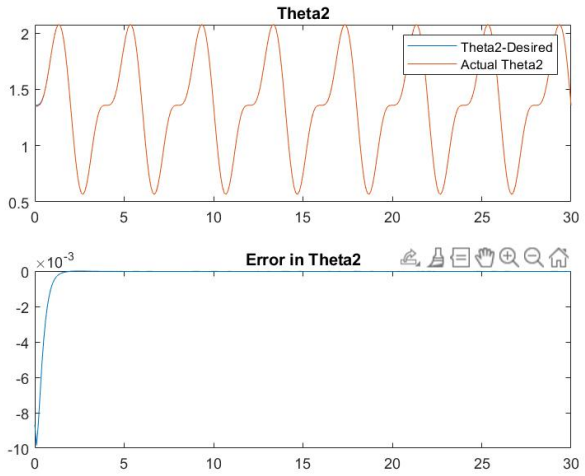

Figure 13: Actual, Desired and Error Plots of θ_2

Robust Controller

In both the previous cases, there was an assumption made that the parameters of the system, $_1$, p_2 and p_3 are known to their true values. This is not the same case in reality. The parameters can never be know to their true values and therefore, their estimates are used. The amount of error in the estimates of the parameters can affect the convergence of the errors to zero and thus, the system's ability to track the desired trajectories is also affected. In this section, it is assumed that the parameters are underestimated such that $\hat{M} = 0.5M$ and $\hat{C} = 0.5C$. Also, the gains are kept same as in the Modified CTC for comparison.

Fig.17, Fig.18, Fig.19 and Fig.20 show the plots of the state variables. It can be seen that unlike the previous 2 controllers, the state variables do not converge to their desired values and thus, the errors never go to zero. Further, the errors oscillate. This happens because the estimates are set to be exactly 50% off from their true values at all times. Therefore, a periodic nature can be seen in the error after some time. Fig.21 shows the plot of input torques.

It has been observed that the amplitude of error plots depend on the values of gains. if the gains are kept low, the amplitude of the oscillation of the error goes high and vice versa is also true. In order to converge the tracking error to zero under the parameter uncertainty, it is necessary to have accurate estimates of the parameters and have the parameter estimation errors converge to zero. This would be discussed in the next section.

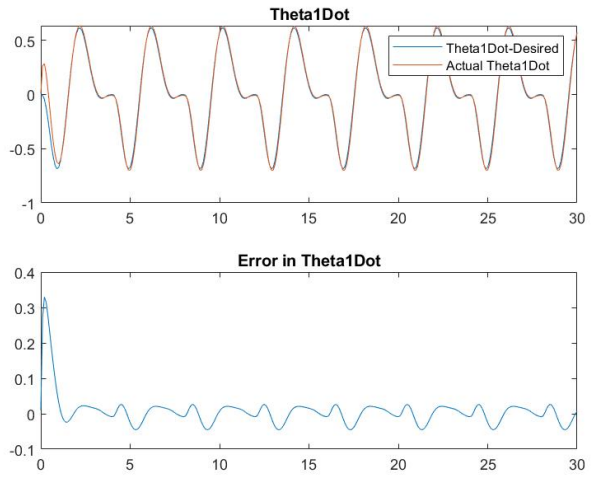

Figure 14: Actual, Desired and Error Plots of $\dot{\theta_1}$

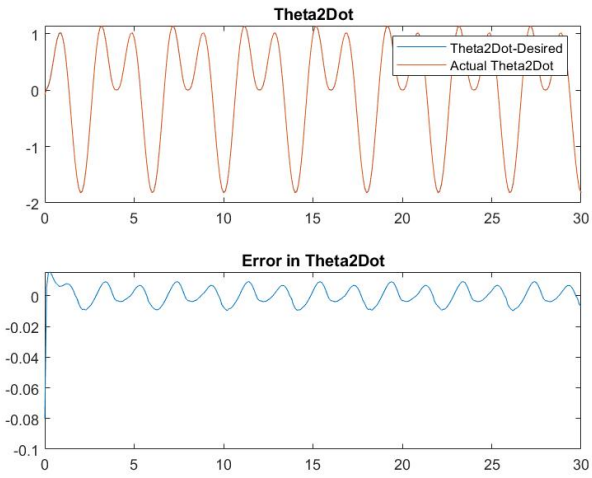

Figure 15: Actual, Desired and Error Plots of $\dot{\theta_2}$

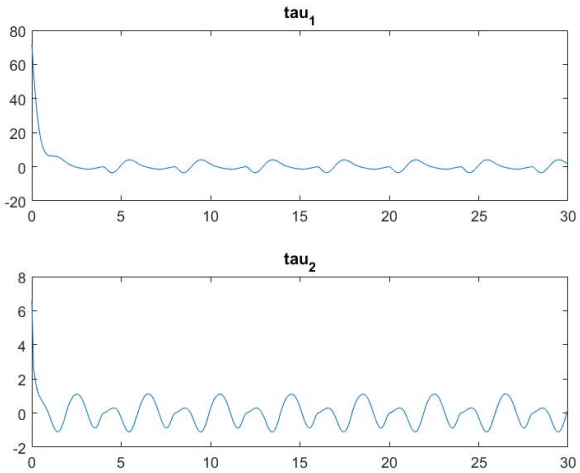

Figure 16: Desired, Actual and Error Plots of τ_1 & τ_2

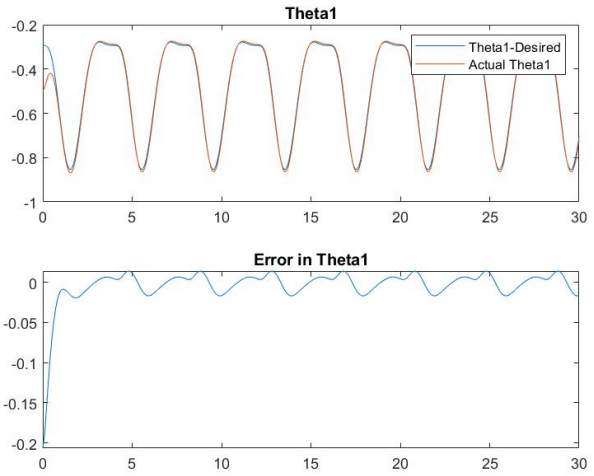

Figure 17: Actual, Desired and Error Plots of θ_1

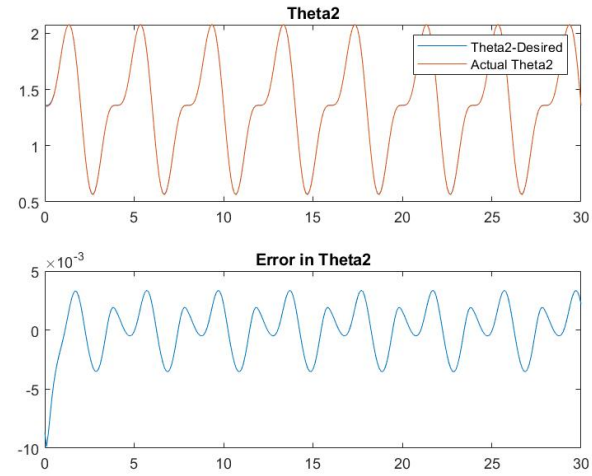

Figure 18: Actual, Desired and Error Plots of θ_2

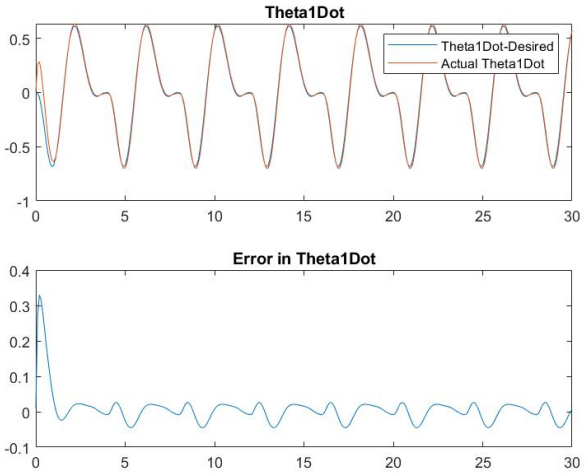

Figure 19: Actual, Desired and Error Plots of $\dot{\theta_1}$

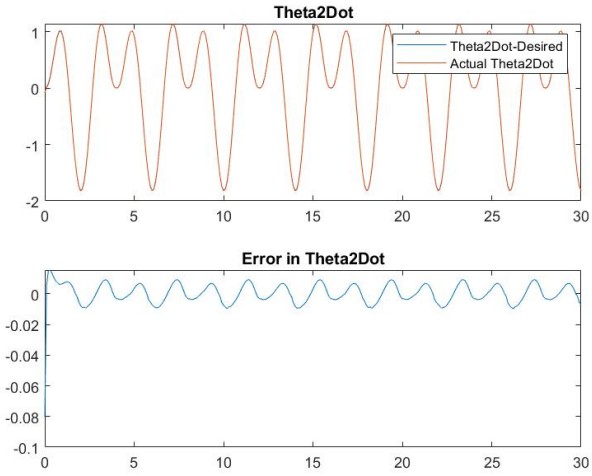

Figure 20: Actual, Desired and Error Plots of $\dot{\theta_2}$

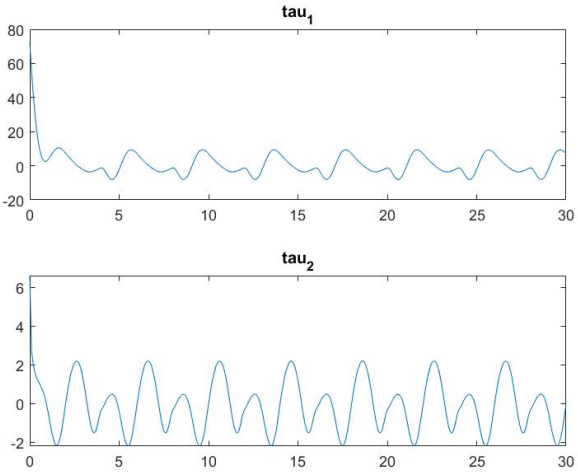

Figure 21: Desired, Actual and Error Plots of τ_1 & τ_2

Adaptive Controller

As mentioned in the previous section, it is important to have accurate estimates of parameters to drive the tracking errors to zero over time. In this controller, parameters are estimated at each time step along with control signals. This gives a better tracking characteristic of the system.

The uncertain parameters of the system are the coupled inertial parameters p_1, p_2 and p_3. Since the matrices M and C depend these inertial parameters, exact values of M and C are unknown at any point of time and thus, its estimates are taken based on the estimates of the inertial parameters p_1, p_2 and p_3.Therefore, input torque can be given as,

$$\tau = \hat{M}(\theta)\ddot{\theta}_r + \hat{C}(\theta, \dot{\theta})\dot{\theta}_r - KS$$

The linear parameterization of the system can be done as shown in the following equations,

$$\hat{M}(\theta)\ddot{\theta}_r + \hat{C}(\theta, \dot{\theta})\dot{\theta} = Y_0 + Y_1\hat{p}_1 + Y_2\hat{p}_2 + Y_3\hat{p}_3$$

For Y_0, $p_1 = p_2 = p_3 = 0 \Rightarrow Y_0 = 0$.

For Y_1, $p_1 = 1$ and $p_2 = p_3 = 0$.

$$\Rightarrow Y_1 = \begin{bmatrix} 1 & 0 \\ 0 & 0 \end{bmatrix} \ddot{\theta}_r + \begin{bmatrix} 0 & 0 \\ 0 & 0 \end{bmatrix} \dot{\theta}_r - Y_0$$

For Y_2, $p_2 = 1$ and $p_1 = p_3 = 0$.

$$\Rightarrow Y_2 = \begin{bmatrix} 0 & 1 \\ 1 & 1 \end{bmatrix} \ddot{\theta}_r + \begin{bmatrix} 0 & 0 \\ 0 & 0 \end{bmatrix} \dot{\theta}_r - Y_0$$

For Y_3, $p_3 = 1$ and $p_1 = p_2 = 0$.

$$\Rightarrow Y_2 = \begin{bmatrix} 2cos(\theta_2) & cos(\theta_2) \\ cos(\theta_2) & 0 \end{bmatrix} \ddot{\theta}_r + \begin{bmatrix} -\dot{\theta}_2 sin(\theta_2) & -(\dot{\theta}_1 + \dot{\theta}_2) sin(\theta_2) \\ -\dot{\theta}_1 sin(\theta_2) & 0 \end{bmatrix} \dot{\theta}_r - Y_0$$

The parameters are estimated as,

$$\hat{p}_1 = -\frac{1}{\gamma_1} S^T Y_1, \quad \hat{p}_2 = -\frac{1}{\gamma_2} S^T Y_2, \quad \hat{p}_3 = -\frac{1}{\gamma_3} S^T Y_3$$

where γ_1, γ_2 and γ_3 are the gains for parameter adaptation. The Lyapunov function candidate can be defined as follows,

$$V = \frac{1}{2} S^T M(\theta) S + \frac{1}{2} \gamma_1 \hat{p}_1^2 + \frac{1}{2} \gamma_2 \hat{p}_2^2 + \frac{1}{2} \gamma_3 \hat{p}_3^2$$

Here, M(θ) is positive definite symmetric matrix. Picking γ_1, γ_2, $\gamma_3 > 0$, it can be seen that V = 0 if and only if S, $\hat{p}_1$, $\hat{p}_2$, $\hat{p}_3 = 0$. Therefore, V is positive definite.

$$\begin{aligned}
\dot{V} &= S^T M(\theta) \dot{S} + \frac{1}{2} S^T \dot{M}(\theta) S + \gamma_1 \tilde{p}_1 \dot{\hat{p}}_1 + \gamma_2 \tilde{p}_2 \dot{\hat{p}}_2 + \gamma_3 \tilde{p}_3 \dot{\hat{p}}_3 \qquad (\tilde{p}_i = \hat{p}_i - p_i, \dot{\tilde{p}}_i = \dot{\hat{p}}_i) \\
&= S^T (M(\theta) \dot{S} + C(\theta, \dot{\theta}) S) + \frac{1}{2} S^T (\dot{M}(\theta) - 2C(\theta, \dot{\theta})) S + \gamma_1 \tilde{p}_1 \dot{\hat{p}}_1 + \gamma_2 \tilde{p}_2 \dot{\hat{p}}_2 + \gamma_3 \tilde{p}_3 \dot{\hat{p}}_3 \\
&= S^T (M(\theta)(\ddot{\theta} - \ddot{\theta}_r) + C(\theta, \dot{\theta})(\dot{\theta} - \dot{\theta}_r)) + \gamma_1 \tilde{p}_1 \dot{\hat{p}}_1 + \gamma_2 \tilde{p}_2 \dot{\hat{p}}_2 + \gamma_3 \tilde{p}_3 \dot{\hat{p}}_3 \\
&= S^T (\tau - C(\theta, \dot{\theta}) \dot{\theta} - M(\theta) \ddot{\theta}_r + C(\theta, \dot{\theta})(\dot{\theta} - \dot{\theta}_r)) + \gamma_1 \tilde{p}_1 \dot{\hat{p}}_1 + \gamma_2 \tilde{p}_2 \dot{\hat{p}}_2 + \gamma_3 \tilde{p}_3 \dot{\hat{p}}_3 \\
&= S^T (\tilde{M}(\theta) \ddot{\theta}_r + \tilde{C}(\theta, \dot{\theta}) \dot{\theta}_r - KS) + \gamma_1 \tilde{p}_1 \dot{\hat{p}}_1 + \gamma_2 \tilde{p}_2 \dot{\hat{p}}_2 + \gamma_3 \tilde{p}_3 \dot{\hat{p}}_3 \\
&= S^T (Y_1 \tilde{p}_1 + Y_2 \tilde{p}_2 + Y_3 \tilde{p}_3 - KS) + \gamma_1 \tilde{p}_1 \dot{\hat{p}}_1 + \gamma_2 \tilde{p}_2 \dot{\hat{p}}_2 + \gamma_3 \tilde{p}_3 \dot{\hat{p}}_3 \\
&= (S^T Y_1 + \gamma_1 \dot{\tilde{p}}_1) \tilde{p}_1 + (S^T Y_2 + \gamma_2 \dot{\tilde{p}}_2) \tilde{p}_2 + (S^T Y_3 + \gamma_3 \dot{\tilde{p}}_3) \tilde{p}_3 - S^T K S
\end{aligned}$$

From the parameters adaptation equations,

$$\begin{aligned}
&\dot{V} = -S^T K S \leq 0 \ \text{ for every S and } \dot{V} = 0 \Longleftrightarrow S = 0 \\
&\dot{V} = -S^T K S \leq -\lambda_{min} K ||S||^2 \\
&\Rightarrow \int_0^t \dot{V}(t) dt \leq \int_0^t \lambda_{min} K ||S||^2 dt \Rightarrow \int_0^t ||S||^2 dt \leq \frac{V(0) - V(t)}{\lambda_{min} K} \leq \frac{V(0)}{\lambda_{min} K}
\end{aligned}$$

$\Rightarrow$ S is square integrable.

$$\begin{aligned}
&V(t) \leq V(0) \\
&\Rightarrow \frac{1}{2} S^T M(\theta) S \leq V(0) \leq \frac{1}{2} \lambda_{min}(M) ||S||^2 \leq V(0) \Rightarrow ||S|| \leq \sqrt{\frac{2V(0)}{\lambda_{min}(M)}} \\
&\Rightarrow \text{S is bounded.} \Rightarrow e \text{ and } \dot{e} \text{ are bounded.} \\
&\Rightarrow \frac{1}{2} \gamma_1 \tilde{p}_1^2 \leq V(0) \Rightarrow |\tilde{p}_1| \leq \sqrt{\frac{2V(0)}{\gamma_1}} \\
&\text{Similarly, } |\tilde{p}_2| \leq \sqrt{\frac{2V(0)}{\gamma_2}} \text{ and } |\tilde{p}_3| \leq \sqrt{\frac{2V(0)}{\gamma_3}}
\end{aligned}$$

Thus, Y_1, Y_2 and Y_3 are bounded. The desired quantities θ_{des}, $\dot{\theta}_{des}$ and $\ddot{\theta}_{des}$ are also bounded by the interpolated function. Thus, the errors e, $\dot{e}$ are bounded. Therefore, $||\ddot{\theta}_r|| = ||\ddot{\theta}_{des} + \lambda e|| \leq ||\ddot{\theta}_{des}|| + \lambda||e||$ is bounded. Therefore, $\dot{S}$ is bounded. As per Barbalat's Lemma, S converges to zero asymptotically and as a result, the errors converge to zero as well.

Fig.22, Fig.23, Fig.24 and Fig.25 show the convergence of state variables and their errors. It can be seen that the error oscillates after decreasing rapidly at the initial time period. The reason for this is the parameters errors being non-zero as can be seen in Fig.27. In Fig.27, it can be seen that the parameters errors ,although not converging to zero in 30s, are approaching zero and will reach zero asymptotically. The input torque plots can be seen in Fig.26. The gains used are as follows,

$$K = \begin{bmatrix} 120 & 0 \\ 0 & 120 \end{bmatrix}, \quad \gamma_1 = 0.5, \quad \gamma_2 = 0.15, \quad \gamma_3 = 0.6$$

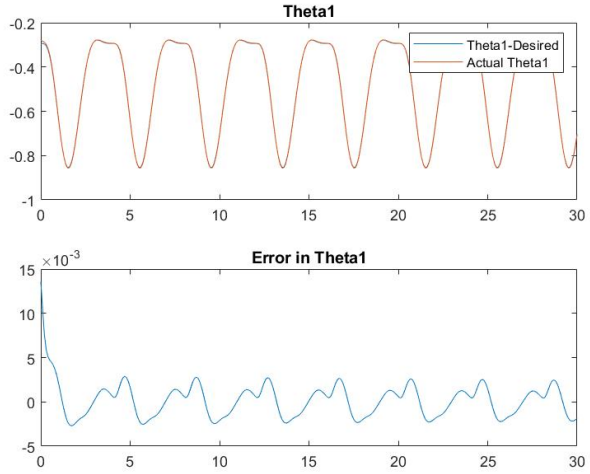

Figure 22: Actual, Desired and Error Plots of θ_1

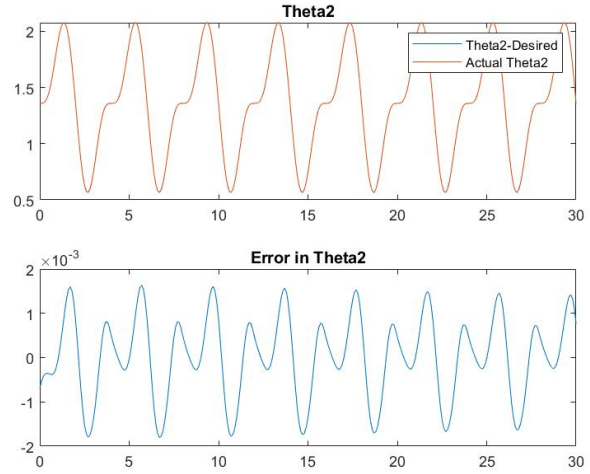

Figure 23: Actual, Desired and Error Plots of θ_2

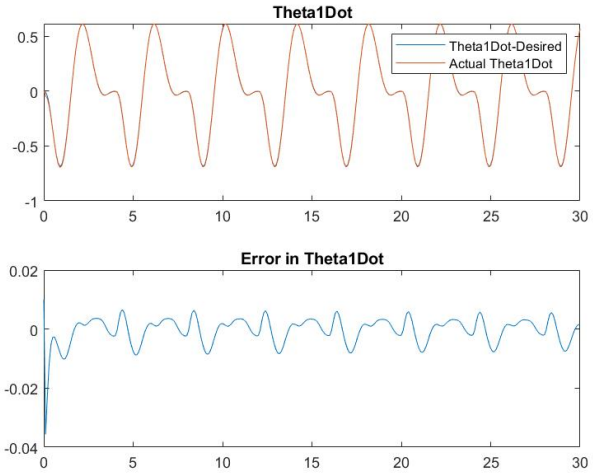

Figure 24: Actual, Desired and Error Plots of $\dot{\theta_1}$

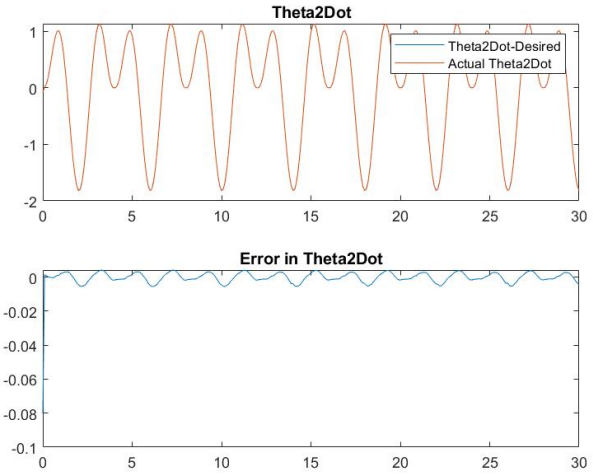

Figure 25: Actual, Desired and Error Plots of $\dot{\theta_2}$

Adaptive Controller with Frictional Parameters

In this case, frictional parameters are considered in the system, but those parameters are uncertain and also their initial values are unknown. An adaptive controller with 3 inertial parameters along with 4 additional friction

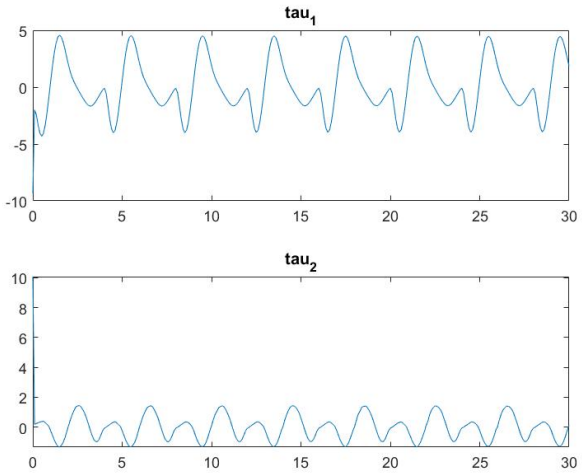

Figure 26: Input Torques τ_1 and τ_2

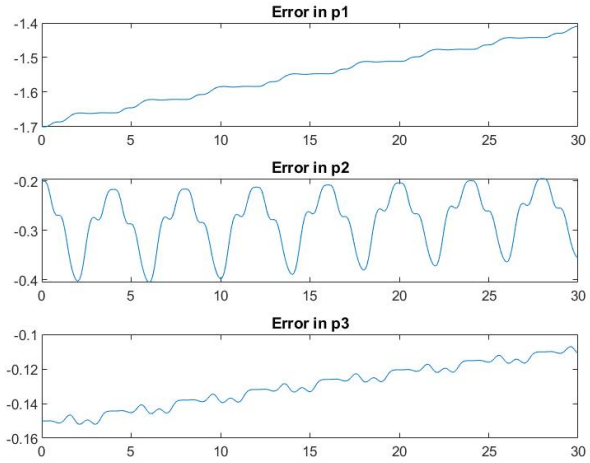

Figure 27: Error in System Parameters p_1, p_2 and p_3

parameters is designed. The equation of motion for the system can be given as,

$$M(\theta)\ddot{\theta} + C(\theta,\dot{\theta})\dot{\theta} + f_{vc}(\dot{\theta}) = \tau$$

$$\text{where,} \quad f_{vc} = \begin{bmatrix} V_1\dot{\theta}_1 + C_1 sgn(\dot{\theta}_1) \\ V_2\dot{\theta}_2 + C_2 sgn(\dot{\theta}_2) \end{bmatrix}$$

The true value of the parameters are $V_1 = 0.4$, $V_2 = 0.2$, $C_1 = 0.2$ and $C_2 = 0.1$. The structure of the simulation is the same as in the previous adaptive controller with 4 more uncertain parameters added to the system. The gains used here are,

$$K = \begin{bmatrix} 90 & 0 \\ 0 & 90 \end{bmatrix}, \quad \gamma_1 = 0.5, \quad \gamma_2 = 0.15, \quad \gamma_3 = 0.6, \quad \gamma_4 = 1.7, \quad \gamma_5 = 1.4, \quad \gamma_6 = 2.5, \quad \gamma_7 = 2$$

Fig.28, Fig.29, Fig.30 and Fig.31 show the plot of the state variables and their errors. Fig.32 and Fig.33 show the parameters estimation errors. Fig.34 shows the input torques required throughout the simulation time.

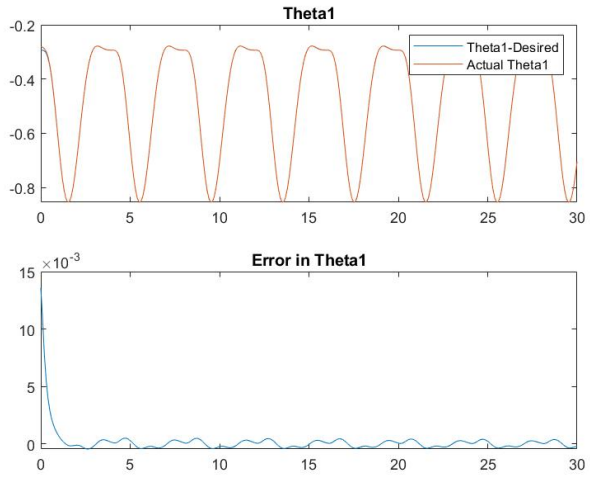

Figure 28: Actual, Desired and Error Plots of θ_1

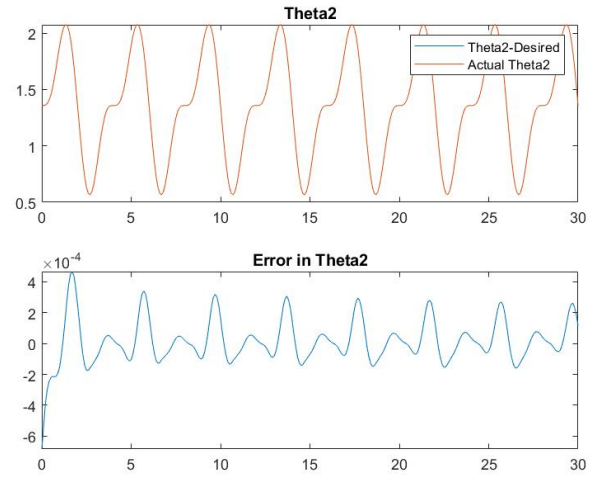

Figure 29: Actual, Desired and Error Plots of θ_2

Discussion

Table 2 shows the norm of tracking errors of the state variables and control input for 30s of simulation. The observations and inferences from the simulation of all the controllers and Table 2 are mentioned below.

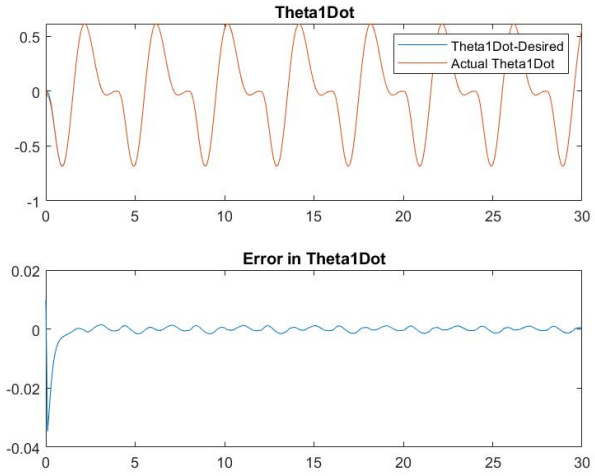

Figure 30: Actual, Desired and Error Plots of $\dot{\theta_1}$

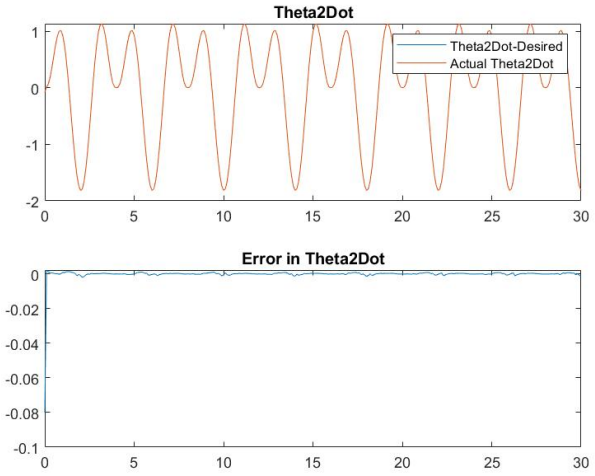

Figure 31: Actual, Desired and Error Plots of $\dot{\theta_2}$

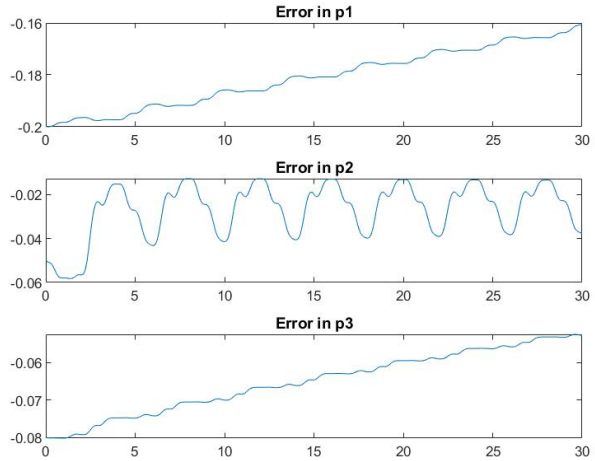

Figure 32: Parameters Errors for p_1, p_2 and p_3

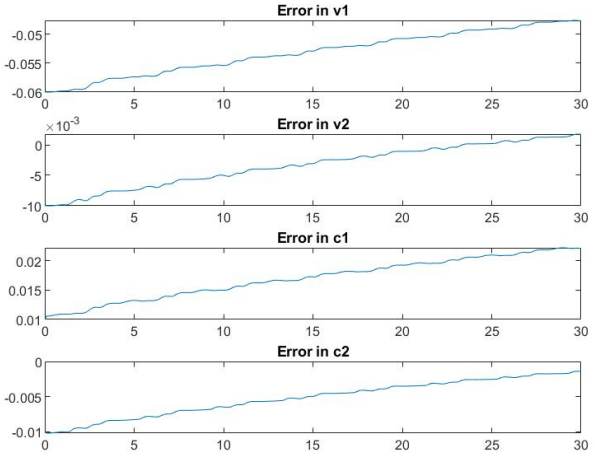

Figure 33: Parameters Errors for V_1, V_2, C_1 and C_2

- It can be observed that the position error is less for PD Controller as compared to Modified Computed Torque Controller. On the other hand, the input torque is much less for PD Controller. This is because K_p and K_d are tuned for optimal convergence time and constrained torque within the available limit. On the other hand, K was used same as K_d for comparison purpose. Further, the convergence time for PD Controller is lesser than that for Modified Computed Torque Controller.

- Robust Controller is a case used to demonstrate the importance of parameter adaptation. The parameters are assumed to 50% underestimated and not been actively estimated with each time time step. It can be observed that this results into high errors and also the highest input torque values out of all the controllers. The result of this controller is bad and also consumes high amount pf power. Thus, real time parameter adaptation is necessary.

- Adaptive Controller performs good and gives small tracking errors. Further, the input torque values are also reasonably smaller than that of controllers without parameter adaptation. The tracking errors would reduce even further when the parameters approach zero after some time. Although, the errors keep oscillating as compared to the errors seen in PD Controller of Modified CTC. This is because of the fact that the parameters also keep changing because they are estimated at each time step. But, overall this controller performs really good as the parameters are initiated with 50% underestimation.

- The errors are even lesser for the adaptive controller with frictional parameters. This is because the gains are tuned for minimal errors and also the frictional parameters are initiated close to their real values. It is

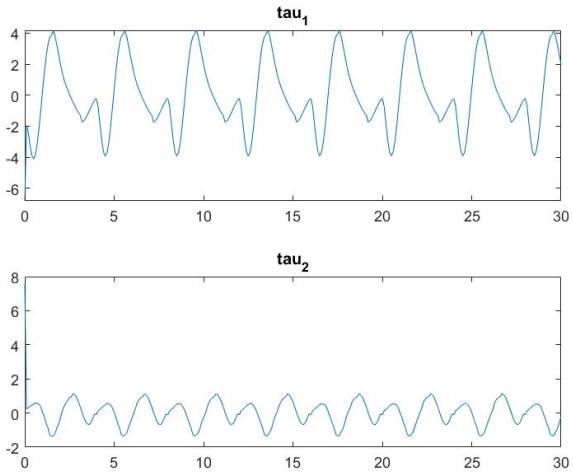

Figure 34: Input Torques for τ_1 and τ_2

Table 2: Norm of Tracking Errors and Input Torques for the Controllers

Controller	θ_1	θ_2	$\dot{\theta}_1$	$\dot{\theta}_2$	τ_1	τ_2
PD Controller	0.2543	0.0164	1.3443	0.1258	85.6407	13.6080
Modified CTC	0.3832	0.0188	0.6507	0.0871	116.0244	13.6746
Robust Controller	0.4071	0.0391	0.7749	0.1266	139.1337	23.2539
Adaptive Controller	0.0347	0.0159	0.0799	0.0915	42.1057	16.9666
Adaptive Controller with Friction	0.0212	0.0025	0.0533	0.0804	39.5083	14.0296

expected to have the errors in the same order as the adaptive controller without frictional parameters if the frictional parameters in this controller are intiated at 50% of their real values.

- To conclude, PD Controllers are simple and widely used, but adaptive controllers provide more reliability and robustness to the system and have a real life application with uncertain situations.